ELSEVIER

Surface Science 423 (1999) 292–302

surface science

Growth and thermal stability of ultrathin films of Fe, Ni, Rh and Pd on the Ru(0001) surface

J. Kołaczkiewicz [a,*], E. Bauer [b,1]

[a] *Instytut Fizyki Doświadczalnej Uniwersytetu Wrocławskiego, pl.M.Borna 9, 50-204Wrocław, Poland*
[b] *Physikalisches Institut, TU Clausthal, 38678 Clausthal-Zellerfeld, Germany*

Received 22 August 1998; accepted for publication 27 November 1998

Abstract

The growth and stability of ultrathin Fe, Ni, Rh and Pd films on the Ru(0001) surface was investigated in the temperature range of 200–2000 K. All films up to a material-dependent thickness agglomerated upon heating to $T>600$ K. At higher temperatures the films differ: Fe and Rh wet the surface again by forming an interfacial alloy, Ni and Pd do not. This indicates that interfacial mixing is determined mainly by electronic rather than by elastic effects.

Keywords: Auger electron spectroscopy; Growth; Low energy electron diffraction (LEED); Low index single crystal surfaces; Metallic films; Work function measurements

1. Introduction

Ultrathin metal films play an important role in science and technology, for example, in heterogeneous catalysis and thin film magnetism. They can always be grown in a layer-by-layer fashion at sufficiently low substrate temperatures as illustrated by the example of Pb films on Si(111) [1] but in many studies and applications the layers have to be stable over a wide temperature range. This is in general not the case because surface, interface and strain energy make the quasi-two-dimensional system unstable towards agglomeration into three-dimensional crystals.

The present study aims at a better understanding of the factors which determine the stability of ultrathin films by comparing the annealing behaviour of four different films of interest in catalysis and ferromagnetism, Fe, Ni, Rh and Pd on a densely packed surface with high symmetry and high surface energy, Ru(0001). The metallic atomic radii of two of the metals, Fe and Ni, differ by ca 8% from that of Ru, those of Rh and Pd very little (0.6 and 1.7%, respectively). Therefore, the misfit influence and the resulting strain energy can be examined by comparing the two metal pairs.

In order to be able to interpret the changes in the measured quantities which occur upon annealing their evolution during growth at various temperatures has to be studied as well. This allows comparison with earlier growth studies [2–7] which were not concerned with stability.

* Corresponding author. Fax: +48 72 3287365; e-mail: kolacz@ifd.uni.wroc.pl.
[1] Present address: Department of Physics and Astronomy, Arizona State University, Tempe, AZ 85287, USA.

0039-6028/99/$ – see front matter
PII: S0039-6028(98)00925-X

2. Experimental

The measurements were carried out in an ultra-high vacuum system with a base pressure of $<1\times10^{-10}$ Torr. The sample was a Ru single crystal whose surface was parallel to the (0001) plane within $\pm0.05^{\circ}$. The sample was cleaned in the manner typical for high melting point metals, that is, by annealing for a few hours in oxygen in the 10^{-7} Torr range, followed by flashing to 2000 K. The cleanness of the sample was checked by Auger electron spectroscopy (AES). Purity evaluation of the sample was difficult due to the coincidence of the Auger signals of Ru and C. Therefore, the commonly employed criterion for the cleanness of a sample, that is the disappearance of the carbon Auger signal, cannot be used in the present case. Two alternate criteria have been used in the past:

1. the minimum value of the 273 eV:183 eV ($M_5N_{23}N_{23}$) signal ratio [8,9]; and
2. the maximum value of the 415 eV ($M_3N_{23}V$):273 eV signal ratio [10,11].

In both cases this value depends on the analyser used, on the primary energy and on the modulation voltage, hence the absolute values cannot be compared. The surface was assumed to be clean when the signal ratio was the same as that cited in Ref. [11]. The temperature of the sample could be varied from 200 to 2000 K and was measured with help of a WRe3%–WRe25% thermocouple spot-welded to it.

The techniques used were AES, low energy electron diffraction (LEED) and work function change ($\Delta\phi$) measurements with the Anderson method. All measurements were made at room temperature after deposition at room temperature or after 1 min annealing at elevated temperatures. The films were deposited cumulatively in successive identical doses, or in single increasingly larger doses. The material was sublimed from pure metal wires wrapped on tungsten wire.

3. Results and discussion

3.1. Fe

The dependence of the 47 eV (M_{23} VV) Fe and of the 273 eV (M_5 VV) Ru Auger amplitudes (AA) (MNN) on the time of deposition at 300 K is shown in Fig. 1. The time dependence indicates initially monolayer-by-monolayer growth. The time intervals t_{i+1}–t_i between the slope changes of the substrate signal are equal and correspond to the time for the formation of 1 ML. The initial slow increase of the Fe Auger signal is due to the fact that the Fe peak is sitting an a steep slope which also changes with deposition time. The slope after completion of the third monolayer is clearly smaller than that expected for monolayer-by-monolayer growth (dashed line) and fits to double layer growth up to t–t_4 . The subsequent scatter is attributed to transition to a more three-dimensional growth.

Annealing at increasingly higher temperatures changes the Auger signals as shown in Fig. 2a for a few layers with thicknesses >2 ML. Layers <1 ML show no changes except those due to desorption. The onset of the changes depends on the layer thickness: the thicker a layer is, the later the changes occur. The local minimum (maximum) of the Fe (Ru) signal, however, always appears

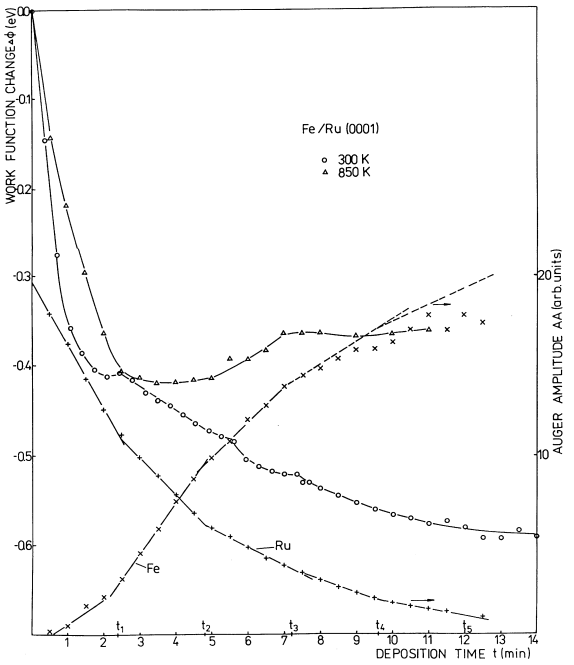

Fig. 1. Dependence of the Auger amplitudes (AA) and work function changes ($\Delta\phi$) on the deposition time.

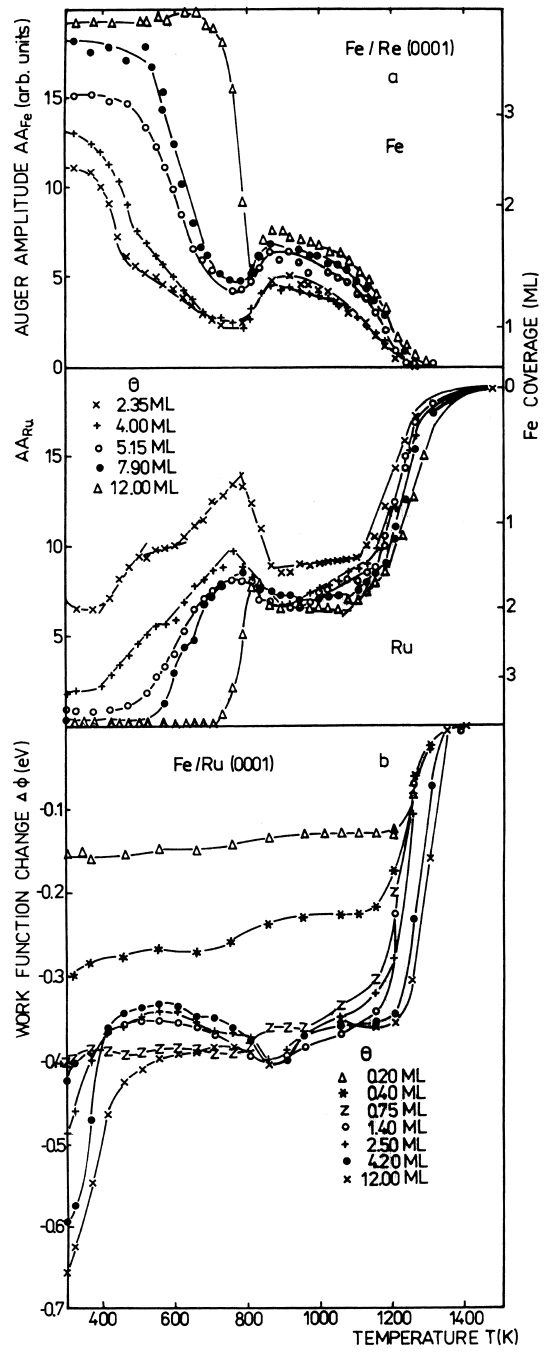

Fig. 2. Change of the AAs of Fe and Ru (a) and the work function change (b) of layers with different thickness with increasing annealing temperature.

at the same temperature, irrespective of the layer thickness. The complicated complementary changes of the Fe and Ru AES signals will be discussed in detail below.

When Fe is deposited at 200 K the LEED pattern does not change except for an increase in the background. Upon deposition at 300 K a (1×1) pattern is seen up to 1 ML. The LEED patterns between 1 and 3 ML have somewhat streaky satellites around the Ru spots (Fig. 3a) which can be attributed to transition structures between the pseudomorphic layer and the (110) oriented Fe layer with bulk periodicity (Fig. 3b) which develops with increasing thickness and/or annealing. The transition patterns (Fig. 3a) were not studied in detail. The pattern of Fig. 3b is from an epitaxial bcc Fe layer with the orientation Fe(110)//Ru(0001) in 3×2 equivalent domains in which the closest-packed atomic rows in film and substrate are parallel. The inter-row misfit is only 0.13% and along the rows the deviation from a 12:11 Fe:Ru coincidence lattice is only 0.075%. The transition from Fig. 3a to Fig. 3b in the thinner layers during annealing is attributed to agglomeration into thicker crystals with 1 ML regions in-between them. Annealing thicker layers above 450 K initially increases the order as expressed in sharper and more intense spots but above 800 K the intensity of the 3x2 Fe(110) domains pattern decreases and at 900 K pattern of Fig. 3c is visible, whose intensity slowly decreases until only the Ru(1×1) spots are left above 1300 K. The pattern of Fig. 3c is visible only for $\theta>4$ ML. For $\theta<4$ ML above 800 K only the (1×1) pattern remains. The pattern of Fig. 3c corresponds to a hexagonal layer with slightly smaller lattice constant than that of Ru. It agrees within the limits of error with that of FeRu ($a=2.626$ Å) and is, therefore, clear evidence of alloying.

The work function changes during deposition at two different temperatures are shown in Fig. 1. The work function decreases at 300 K, though, an inflexion of the curve is visible $\theta=1$ ML, at and saturates than for $\theta>5$ ML. The saturation value $\phi=4.92$ eV [assuming $\phi=5.4$ eV for the clean Ru(0001) surface [3,4]] is in reasonable agreement with that of 4.81 eV reported for the clean Fe(110) surface [12]. Upon deposition of one single large

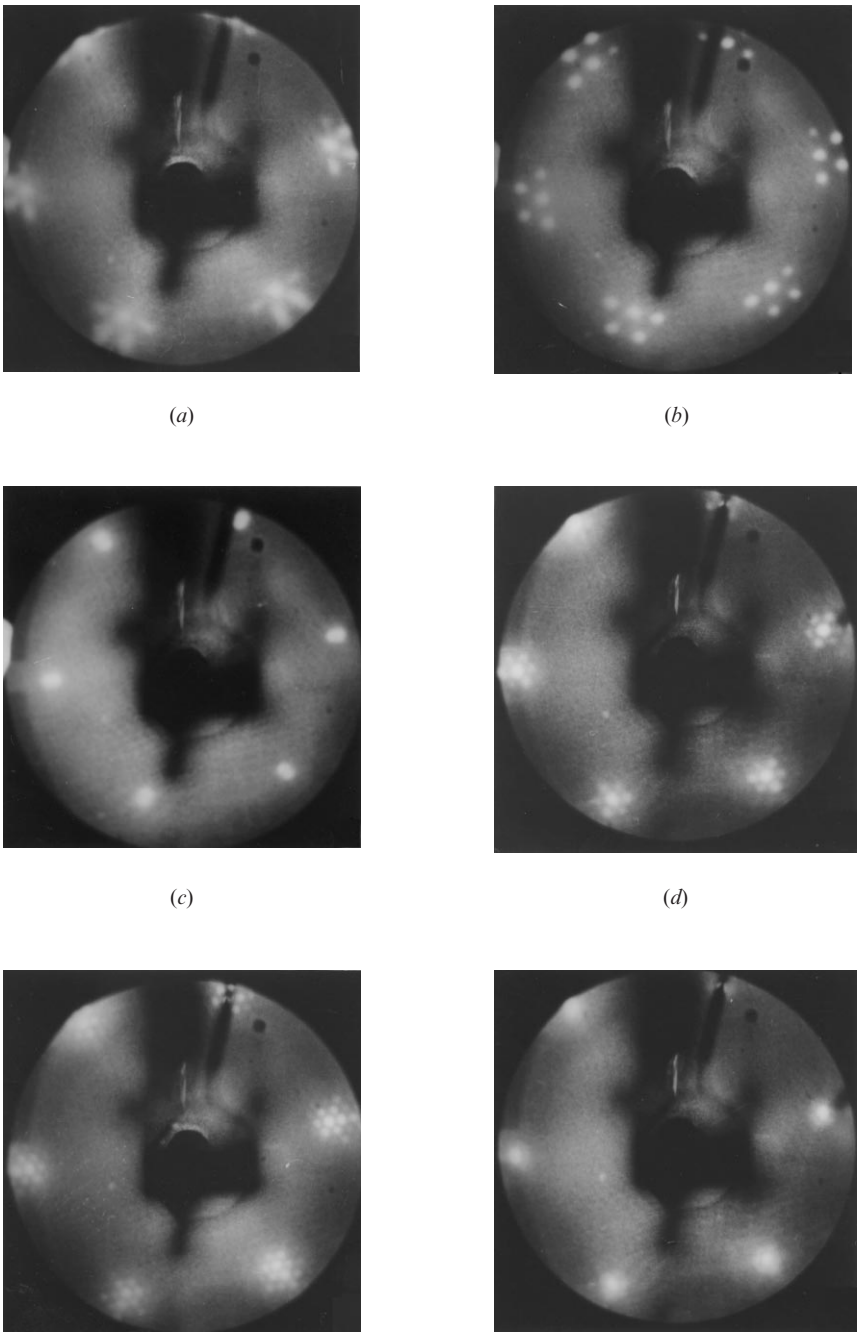

(*a*) (*b*)

(*c*) (*d*)

(*e*) (*f*)

Fig. 3. Observed (LEED) patterns. (a) Fe: $\theta = 2.1$ ML, Ep = 84 eV, $T = 300$K; (b) Fe: $\theta = 4.2$ ML, Ep = 99.4 eV, $T = 970$ K; (c) Fe: $\theta = 4.2$ ML, Ep = 102 eV, $T = 1170$ K; (d) Ni: $\theta = 0.85$ ML, Ep = 80.7 eV, $T = 300$ K; (e) Ni: $\theta = 1.8$ ML, Ep = 83.7 eV, $T = 1050$ K; (f) Ni: $\theta = 0.65$ ML, Ep = 80.7 eV, $T = 1050$ K (T are the annealing temperatures).

dose the work function change is ~0.1 eV greater. The $\phi(\theta)$ changes at $T=950$ K are different: between 1 and 2 ML the work function has a broad minimum, then it increases by 0.03 eV to reach a value ~5 eV at $\theta=3$ ML.

Heating layers deposited at 300 K to increasingly higher temperatures causes changes of the work function as illustrated in Fig. 2b for several coverages. In layers with $\theta<1$ ML only a small increase of the work function, <0.03 eV, was noticed at $T=800$ K. In thick layers the work function decreases between 600 and 850 K by ~0.05 eV after a strong initial rise from the 300 K value. The work function at the minimum of the $\Delta\phi(\theta)$ curve at $T=850$ K at $\theta>1$ is independent of the layer thickness. The minimum is associated with the vanishing of the pattern inFig. 3b and the appearance of the pattern in Fig. 3c, which corresponds to the transition from the bcc(110)Fe layer (Fig. 3b) to the hexagonal layer (Fig. 3c).

Although Fe grows on the Ru(0001) surface at $T=300$ K initially ML-by-ML, thicker layers agglomerate upon heating except for the first monolayer (see Fig. 2a). Up to 4 ML the agglomeration occurs in two steps, the first one from 300 to ~500 K, the second one starting at ~600 K. Agglomeration terminates up to 4 ML at 740 K. The Fe crystals must be quite large because the Fe Auger signal corresponds to 1 ML so that the crystals can cover only a small fraction of the surface. The rapid changes of the Fe AES signal at ~5 and 8 ML also extrapolate to 740 K but the 1 ML level is not reached because of the larger coverage of the three-dimensional crystals. Above 800 K spreading of Fe starts as seen in the decrease (increase) of the Ru (Fe) Auger signals. This is attributed to interfacial alloying which reduces the interface energy and changes the equilibrium shape of the Fe crystals from a more three-dimensional to a flat shape with larger width. Above ~880 K the Fe signal decreases again and the Ru signal increases slightly in the thinner films ($\theta<4$ ML) but remains more or less constant in the thicker films ($\theta>4$ ML). This can be attributed to propagation of the alloy from the interface through the Fe crystals so that Fe–Ru alloy crystals form. Above 1100 K both Auger signals change faster which can be seen particularly well in the thicker layers. This is undoubtedly due to desorption of Fe which leaves only ~1 ML at 1200 K in the thinner layers at the annealing times used. Above 1200 K the first monolayer also desorbs. The change in work function at this temperature, however, does not give much information on the processes occurring.

The results obtained for the growth of Fe are in agreement with more recent studies of this system [13,14] but agree only partially with those of the first study [2–4]. In Ref. [2] only the pattern p(1×1) was observed, whereas in Refs [3] and [4] the complex LEED pattern (Fig. 3b) was attributed to a layer of Fe(110) such that [110]Fe(bcc)//[120]Ru(hcp). References [13] and [14] and the present studies show growth of three-dimensional Fe crystals in a Kurdyumov–Sachs orientation ([1$\bar{1}$1](bcc)//[110]fcc), in this case ([1$\bar{1}$1](Fe)//[10$\bar{1}$0]Ru). Furthermore, the lattice constant difference between Ru and Fe–Ru alloy obtained upon annealing was not previously noted.

3.2. Ni

The dependence of the Ni 61 eV (M_{23} VV) AA and of the Ru 273 eV (M_5 VV) AA on the deposition time are shown in Fig. 4 together with $\Delta\phi(\theta)$. The room temperature AA(t) of film and substrate vary in a manner characteristic for monolayer-by-monolayer growth. During deposition at 800 K the AA increases linearly only in the first segment. Further deposition causes only a small additional increase.

The effect of annealing on the Auger signals is shown in Fig. 5a. Up to 1 ML the signals are constant until desorption sets in at ~1100 K. Above 1 ML desorption is preceded by agglomeration or alloying where the onset temperature depends upon the thickness: from ~600 K at 1.8 ML to ~900 K at 3.55 ML. Interestingly, at coverages slightly exceeding 1 ML, for example, at 1.2 ML, this process is somewhat delayed.

At the lowest coverages a (1×1) LEED pattern is observed. Above $\theta=0.5$ a pattern with six extra spots surrounding the Ru spots appears (Fig. 3d) whose intensity increases with coverages up to $\theta=$ 1 ML. At this coverage the other extra spots reach an intensity comparable with that of the Ru spots.

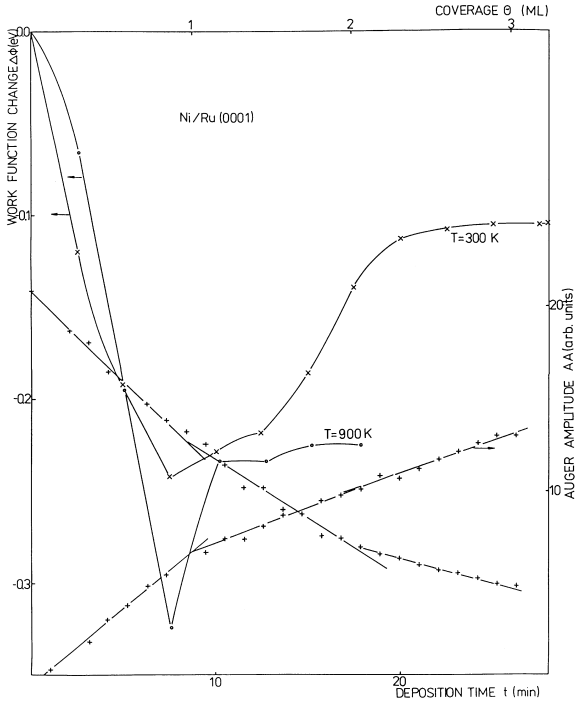

Fig. 4. Dependence of the AAs and $\Delta\phi$ of Ni layers on deposition time.

They agree within 0.5% with those of a superimposed Ni(111) plane with bulk interatomic distances. At $\theta > 1$ ML additional multiple scattering spots appear and the lattice constant of the hexagonal overlayer increases by $\sim 1\%$ as seen in Fig. 3e. Annealing below ~ 800 K increases the sharpness of this pattern. Above 800 K the intensity of these spots decreases until only the six spots closest to the Ru spots remain with an intensity corresponding to that of the 1 ML pattern. Heating the layers with $\theta < 1$ ML > 600 K results in the decay of the additional spots surrounding the Ru spots, to be replaced by rings (Fig. 3f) which disappear with increasing temperature, too; only the (1×1) pattern remains. The disappearance temperature of the rings increases with increasing coverage from ~ 900 K for $\theta = 0.8$ ML to 1250 K for $\theta =$ 2.5 ML. The changes in the diffraction pattern are reflected in the Auger signals which are close to the 1 ML level between 800 and 1100 K (coverage-dependent). Deposition at 200 K leads to an

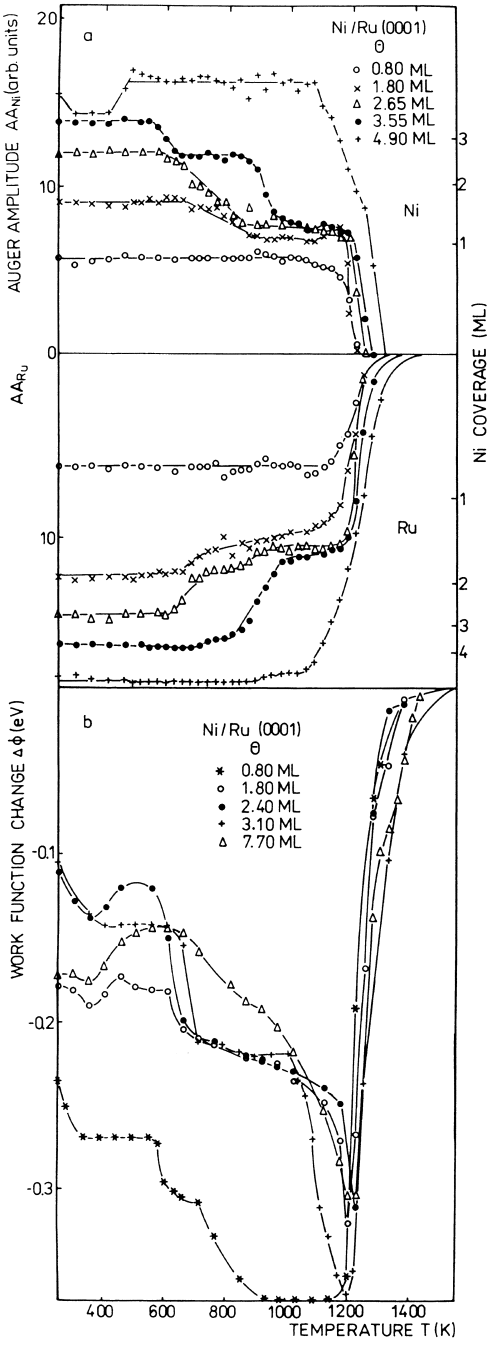

Fig. 5. Change of the AAs of Ni and Ru (a) and work function change (b) with annealing temperature at several coverages.

increase of the background and makes the (1×1) spots diffuse.

The work function changes measured during

deposition at 300 and 900 K are shown in Fig. 4. At 900 K the work function has a deep minimum below 1 ML, and saturates $\sim$1 ML. At 300 K the minimum is much less pronounced and ϕ increases again with some delay after 1 ML to a saturation value of $\Delta\phi = -0.1$ eV. The difference in the depth of the submonolayer minimum is attributed to the irreversible transition from non-equilibrium close-packed Ni islands to pseudomorphic islands with lower packing density and, therefore, lower work function, similar to the case of Ni and Co on Mo(110) [12]. Heating of the Ni layers deposited at 300 K results in marked work function changes (Fig. 5b). The extent of the changes depends on coverage: below 1 ML ϕ decreases strongly up to 1000 K – reflecting the increasing transition from the close-packed to the pseudomorphic structure which apparently occurs in two steps (600 and 750 K) – and then increases due to Ni desorption. Above 1 ML the largest changes are observed between 600 and 800 K at $\theta = 2$ ML which indicates strong agglomeration of the second monolayer. At 3.55 ML agglomeration does not start until 800 K and at 4.9 ML the layer is stable until the onset of desorption at $\sim$1100 K as seen in the Auger signals (Fig. 5a). The first decrease of ϕ between 600 and 800 K is connected with the change in Auger signals mentioned before and in the LEED patterns in which the pattern Fig. 3e is replaced by the pattern of Fig. 3d as expected from the increase of the thickness of the Ni crystals which leaves the monolayer in-between them. The work function decrease at $T = 1100$ K is associated with the transition of the LEED pattern of Fig. 3f to a (1×1) pattern.

At $700 < T < 1100$ K the value of $\Delta\phi$ for $1 < \theta < 3$ ML is equal to that observed during the deposition at 900 K, which corresponds to a monolayer coverage. Above 3 ML the $\Delta\phi$ values increase with coverage, which may indicate the formation of a surface alloy, whose work function increases with increasing concentration of Ni in the alloy.

Although Ni grows on Ru(0001) at room temperature in the layer-by-layer mode layers >1 ML are not stable but agglomerate upon heating into islands which are so thick that the multiple scattering pattern is replaced by the 1 ML LEED pattern and that the Auger signals of film and substrate nearly have 1 ML values. The large work function changes between 600 and 800 K parallel the changes in the Auger signals (Fig. 5). After annealing to 700 K the first layer is pseudomorphic based on the disappearance of additional spots.

The growth results obtained agree well with those of Ref. [5] which reports data on the growth at 100 and 700 K. The saturation value of the work function 5.3 eV, assuming $\phi_{Ru} = 5.4$ eV, is between the value 5.2 eV [15] of the bulk Ni(111) surface and the value 5.43 eV of thick Ni layers on Mo(110) [12].

3.3. Rh

In the case of rhodium relatively few measurements were made because it is difficult to remove Rh from the substrate by thermal treatment within an acceptable time. The dependence of the 302 eV (M_5 NN) Rh and substrate Auger signals upon deposition time is shown in Fig. 6. The slopes of the linear segments changes after equal time intervals corresponding to the completion of successive monolayers.

Fig. 7a shows how the Rh and Ru Auger signals change upon annealing. In layers <1 ML thick no changes have been noted apart from those connected with the desorption of Rh. Significant changes occur, however, at higher coverages which are interpreted as follows. The brief initial rise of the Rh signal seen at some coverages are attributed to smoothing of the atomically rough as-grown layer surface. After levelling off or slightly increasing (decreasing) the Rh (Ru) signals decrease (increase) above a coverage-dependent temperature ranging from about 550 K for $\theta < 2$ via about 750 K at $\theta = 2.5$ and 3.3 to ca 900 K at $\theta = 4$. These changes can be explained by agglomeration of the Rh layer. Starting at about 970 K in the thinner layers the Rh (Ru) signals increase (decrease) again indicating spreading of the Rh layer. This wetting process is attributed to interfacial alloying and is best seen at 2.5 ML. It partially overlaps with the delayed agglomeration process at 4 ML and completely overlaps with it at $\theta > 5$ ML so that the signals remain constant up to 1200 K. The stronger changes above ca 1270 K are due to desorption

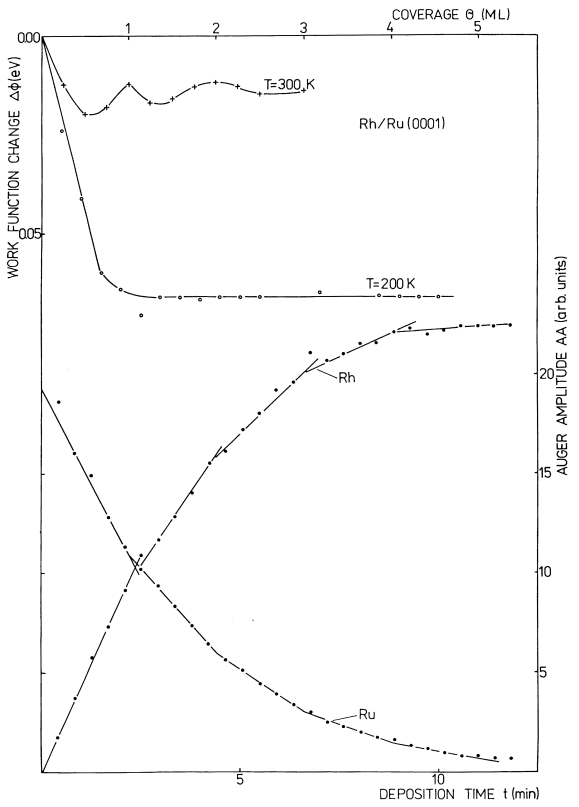

Fig. 6. Dependence of the AAs of Rh and Ru and of $\Delta\phi$ on the deposition time of Rh.

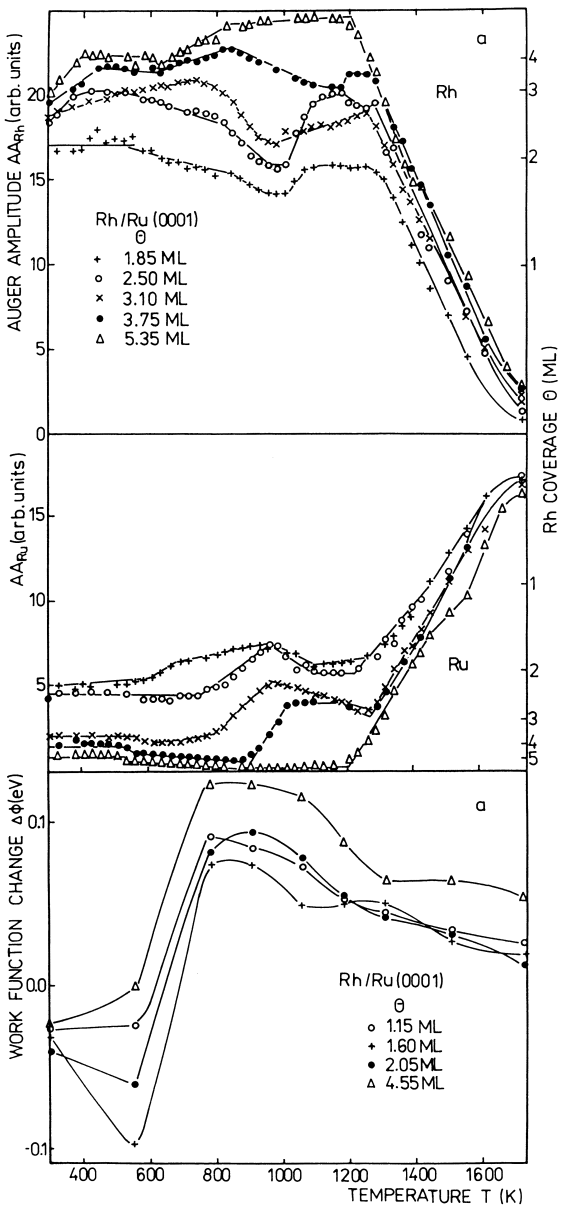

Fig. 7. Change of the AAs of Rh and Ru (a) and work function change (b) of layers with different thickness with annealing temperature.

which is still incomplete at 1700 K as seen by the residual Rh signal.

LEED shows that Rh grows at room temperature pseudomorphically in the entire coverage range investigated ($\theta < 5$ ML). Deposition at 200 K also produces a (1×1) pattern as does annealing up to the deposition temperature.

The work function varies only little during Rh deposition. At 300 K two maxima occur at the completion of the first two monolayers in agreement with the monolayer-by-monolayer growth seen in AES but on average $\Delta\phi$ is only -0.015 eV. Deposition at 200 K reduces ϕ by 0.065 eV already at 1 ML, a value which remains constant up to the highest coverages indicating constant roughens of the layer during growth. Annealing causes more pronounced changes of the work function (Fig. 7b). It decreases initially to a minimum value upon heating to 600 K, from which it increases rapidly by as much as ca 0.3 eV upon heating to 800 K. This is several times more than the changes noted during deposition at 300 K. Further heating causes a gradual decrease of the work function towards the value of the clean

substrate. As seen in Fig. 7b the temperature and annealing time used in this experiment was insufficient for complete desorption. The magnitude of the changes induced by annealing depends on the layer thickness, the larger changes occurring between 1 and 2 ML. The initial decrease of the work function can be attributed to H_2 desorption at 500 K, the increase at 600 K is connected with the smoothing of the layer. The work function values for Ru and Rh are 4.6 and 4.75 eV, respectively [15], in good agreement with the measured maximum $\Delta\phi$ value 0.1 eV.

3.4. Pd

As in the former cases, the 300 eV (M_5 NN) Auger signal of Pd and that of the substrate change piecewise linearly with breaks at equal time intervals (Fig. 8a). The substrate signal does not vanish with increasing film thickness because Pd has also an Auger peak at 271 eV which overlaps with the Ru peak. The Auger signals of layers with $\theta<1$ do not change upon annealing up to the desorption temperature. In layers with $\theta>1$ the ratio of the Auger signals decreases above a thickness-dependent temperature ranging from 450 K at $\theta=1.35$ via 570 K at $\theta=1.75$, 850 K at $\theta=2.75$ to 940 K at $\theta=4.15$ (Fig. 9a). This decrease is attributed to agglomeration of the layer. The process occurs in two steps, the second one starting at 820 K for $\theta<2$ and 900 K for $\theta=2.75$. At $\theta>4$ ML only one step is seen and at still higher coverages agglomeration does not occur until desorption sets in at ca 1100 K.

LEED shows independent of coverage and annealing temperature a (1×1) pattern, in the deposition at 200 K with a strong background.

Deposition at 200 K (Fig. 8a) reduces the work function by 30 meV whereas deposition at 300 K increases the work function. This increase is small in the first monolayer (35 mV), but rises thereafter rapidly by 0.16 eV to a saturation value at $\theta>3$. Assuming $\phi=5.4$ eV for Ru(0001), this $\Delta\phi$ change the corresponds to $\phi=5.56$ eV which is the work function of the clean Pd (111) surface. Fig. 8b shows work function changes which were measured at room temperature for two different doses under conditions of palladium contamination by

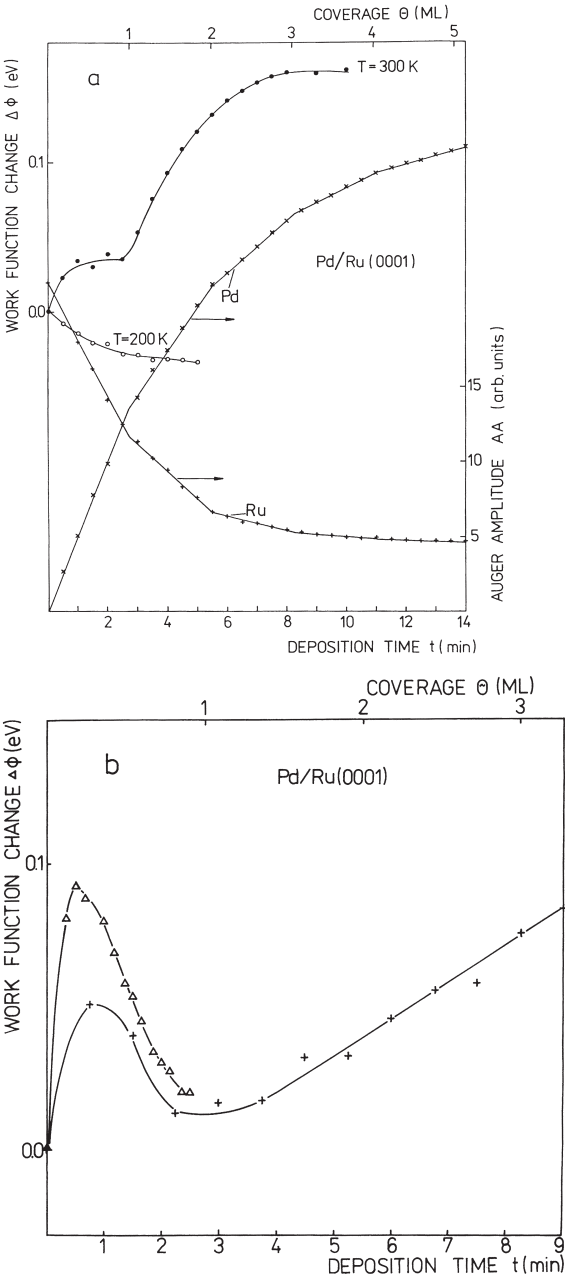

Fig. 8. Dependence of the AAs of Pd and Ru and of $\Delta\phi$ (a) and $\Delta\phi$ with H_2 coadsorption (b) on the deposition time of Pd.

hydrogen. During this Pd deposition hydrogen was liberated in amounts well in excess of the background level (the palladium source remained switched off (was not heated) for some prolonged

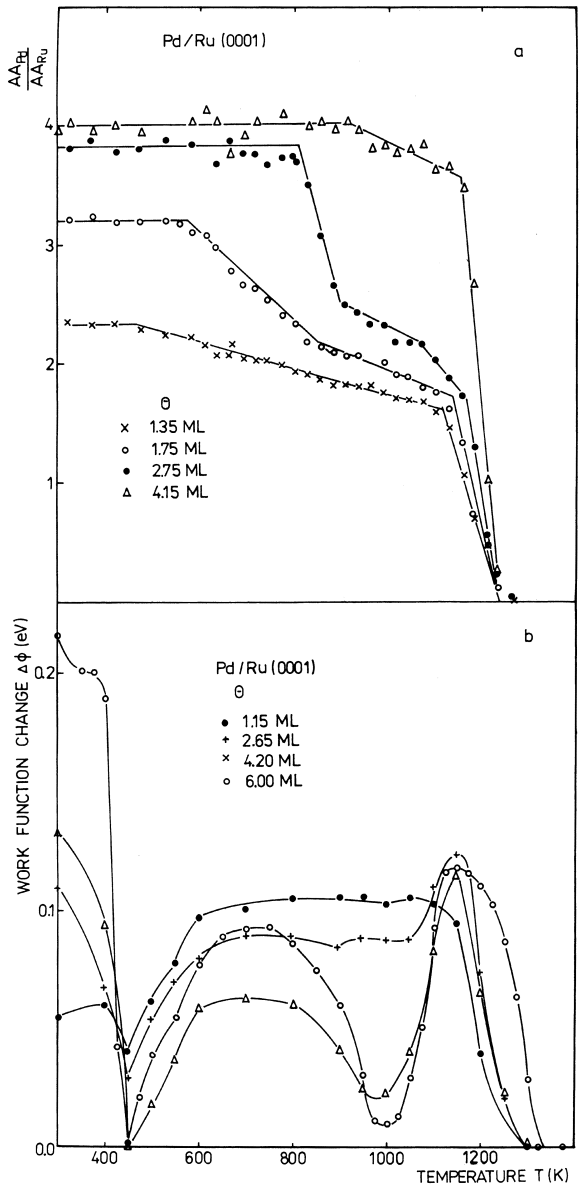

Fig. 9. Change of the AA ratio of Pd to Ru (a) and work function change (b) with annealing temperature for Pd layers.

period in the vacuum apparatus, which resulted in contamination of the source by hydrogen). The work function has pronounced maximum at $\theta = 0.2$ ML and a minimum at 1 ML. The minimum work function at 1 ML is slightly lower than in Fig. 8a. At higher coverages the work function increases like in Fig. 8a.

Annealing the Pd layers leads to relatively complicated changes of the work function as shown in Fig. 9b. In the entire coverage range a strong decrease up to 450 K is seen. This is attributed to desorption of adsorbed hydrogen. The maximum of the $\Delta\phi(T)$ curves at 700 K is connected with the smoothing of the Pd layer. The decrease above 800 K in the thinner layers is due to the onset of agglomeration, while the rapid decrease above 1100 K is due to desorption of palladium. The minimum value of work function in the curves for $\theta > 1$ ML at 1000 K is quite close to the value measured during the deposition at 1 ML (Fig. 8b). The maximum at 1150 K, can not be attributed to hydrogen as in Fig. 8b but may be due to alloying in the submonolayer range at high temperature.

Palladium grows on the Ru(0001) surface pseudomorphically. The first monolayer is thermally stable whereas the subsequent layers agglomerate upon heating into isolated crystals which do not affect the LEED patterns. The work function changes at 300 K below 1 ML give no indication of a two-dimensional gas which was reported for Ag on the Ru(0001) surface [16]. The work function decrease at 200 K is due to the disorder in the layer whose roughness dominates the slight increase of ϕ which accompanies the Pd adsorption in the submonolayer range. These LEED and AES(θ) results are in good agreement with those reported in Ref. [6].

4. Summary

In the submonolayer region of all layers no evidence was found for formation of the chain structures observed on W(110) [17] in the temperature range studied although the dipole–dipole interaction is much weaker than that in the case of the same metals on the W(110) surface. This is due to the fact that on the Ru(0001) surface the polarization or the charge transfer to the substrate is insignificant. The values of the dipole moments of Fe, Ni, Rh and Pd atoms are $\mu = 0.13$, 0.17, 0.018 and -0.044 D, respectively. The small dipole moment makes it difficult to observe the two-dimensional gas–condensate phase transition

which occurs in the submonolayer range at high temperatures unless it is preempted by desorption.

The structure of the first monolayer is pseudomorphic for all the adsorbates except Ni; the subsequent layers are pseudomorphic, too, for the elements whose atomic radius is close to that of the substrate (Rh, Pd). When the atomic radii differ strongly (Fe, Ni) the layers rapidly approach their bulk structure. In all metals investigated agglomeration of the material in excess of one monolayer has been observed, with a thickness-dependent onset temperature. Very thick layers ($\theta > 10$ ML) do not agglomerate before alloying with the exception of Fe.

An interesting result of this study is that interfacial mixing (wetting)occurs in Rh and Fe layers but appears to be absent in Pd and Ni layers. This clearly eliminates the difference in atomic size or misfit as driving force for wetting because Rh differs little from Ru and wets while Ni differs strongly in atomic size from Ru and does not wet. This shows that wetting is not strain-driven, that is not of elastic origin but rather driven by chemical, that is, electronic interaction. Apparently, elements with less filled three-dimensional shells have a stronger tendency to interfacial alloying – which is believed to mediate wetting – with Ru than elements with more filled three-dimensional shells.

Acknowledgements

This work was carried out at the Physikalisches Institut, Technische Universitaet Clausthal within a DFG-supported collaboration between this and the first authors institute. Partial support by the Polish State Committee of Scientific research (KBN) Grant No. PB/1346/P03/97/12.

References

[1] M. Jałochowski, M. Hoffmann, E. Bauer, Phys.Rev. B 51 (1995) 7231.
[2] C. Liu, S.D. Bader, Phys.Rev. B 41 (1990) 553.
[3] C. Egawa, T. Agura, Y. Iwasawa, Surf. Sci. 185 (1987) L506.
[4] C. Egawa, T. Agura, Y. Iwasawa, Surf. Sci. 188 (1987) 563.
[5] P.J. Berlowitz, J.E. Houston, J.M. White, D.W. Goodman, Surf. Sci 205 (1988) 1.
[6] C. Park, Surf. Sci 203 (1988) 395.
[7] J.A. Rodriguez, R.A. Campbell, D.W. Goodman, Surf. Sci 307–309 (1994) 377.
[8] J.T. Grant, T.W. Haas, Surf. Sci 21 (1970) 76.
[9] P.D. Reed, C.M. Comrie, R.M. Lambert, Surf. Sci. 59 (1976) 33.
[10] T.E. Madey, H.A. Engelhardt, D. Menzel, Surf. Sci. 48 (1975) 304.
[11] J.S. Badyal, A.J. Gellman, R.M. Lambert, Surf. Sci. 188 (1987) 557.
[12] M. Tikhov, E. Bauer, Surf.Sci 232 (1990) 73.
[13] S. Andrieu, M. Piecuch, J.F. Bobo, Phys.Rev. B 46 (1992) 4909.
[14] D. Tian, H. Li, F. Jona, P.M. Marcus, Solid State Commun. 80 (1991) 783.
[15] V.S. Fomenko, I.A. Podtshernaijeva, Emissionnyje i adsorbtionnyje svojstva materialov, Atomizdat, Moscow, 1975.
[16] M. Nohlen, M. Schmidt, H. Wolter, K. Wandelt, Surf. Sci 337 (1995) 294.
[17] J. Kołaczkiewicz, E. Bauer, Phys.Rev. B 44 (1991) 577.